Spatial Vision, Vol. 12, No. 1, pp. 31–50 (1999)

Spatial frequency and visual persistence: Cortical reset

GREGORY FRANCIS *

Department of Psychological Sciences, Purdue University, 1364 Psychological Sciences Building, West Lafayette, IN 47907-1364, USA

Received 2 November 1997; revised 7 July 1998; accepted 10 July 1998

Abstract—Psychophysical studies show that the duration of visual persistence increases with spatial frequency of gratings. Previous theories ascribe this finding to differences between the spatial and temporal properties of sustained and transient pathways. This paper proposes an alternative account that explains persistence as a side-effect of excitatory feedback in neural circuits for contour extraction. Mechanisms to break excitatory feedback include inhibitory reset signals at stimulus offset. Simulations demonstrate how gratings with lower spatial frequency generate stronger inhibitory reset signals, thereby resulting in shorter persistence for lower spatial frequencies. Additional simulations account for interactions of spatial frequency with stimulus duration, effects of adaptation, and properties of residual traces, as opposed to visual persistence.

INTRODUCTION

Brief visual stimuli often seem to last much beyond their physical duration so that stimuli as brief as 5 ms seem to last more than 300 ms (e.g. Bowen *et al.*, 1974). The duration of persistence is related inversely to stimulus duration (Bowen *et al.*, 1974), inversely to stimulus intensity (Bowen *et al.*, 1974), inversely to proximity of a nearby stimulus (Farrell *et al.*, 1990), and directly to stimulus spatial frequency (Meyer and Maguire, 1977).

Francis *et al.* (1994) accounted for all of these factors, except spatial frequency, with a neural network model of visual perception. In the model, persistence is the result of lasting neural responses that derive from excitatory feedback in cortical neural circuits. Mechanisms embedded in the neural circuits inhibit lasting responses generated by a stimulus, thereby preventing neural responses from persisting too long. One mechanism was lateral inhibition, which had spatial properties that accounted for inverse-proximity effects. A second mechanism

*E-mail: gfrancis@psych.purdue.edu

created reset signals at stimulus offset that actively inhibited subsequent responses generated by the stimulus. Increases in stimulus duration and luminance increased the strength of the reset signals and thereby decreased persistence, in agreement with the psychophysical data.

This article shows how simulations of the model that include filters of multiple sizes account for the relationship between persistence and spatial frequency. Simulations of the model account for the following psychophysical data:

- Spatial frequency: for bar and sine gratings, visual persistence is directly related to spatial frequency. Likewise, persistence is inversely related to the size of a single bar (Meyer and Maguire, 1977, 1979).
- Frequency and duration: high frequency gratings show a strong inverse relationship between persistence and stimulus duration. Low frequency gratings have a weaker inverse duration effect (Meyer and Maguire, 1981).
- Pretest adaptation: for a high frequency grating with short durations, pretest adaptation to that grating reduces persistence. Persistence is unchanged for gratings of long duration, and for low frequency gratings (Meyer and Maguire, 1981).
- Residual traces: when observers judge the offset of any residual trace of the target grating, the duration of the trace is inversely related to spatial frequency (Long and Sakitt, 1981).

In the model, the effects of stimulus duration, spatial frequency, adaptation, and residual traces depend on the behavior of cortical reset signals. The next section briefly describes the model and the mechanisms underlying visual persistence.

MULTIPLE SCALES IN THE BOUNDARY CONTOUR SYSTEM

The model, called the Boundary Contour System (BCS), consists of a large set of individual neurons with excitatory and inhibitory connections that promote computations necessary for visual perception. Since Grossberg (1994) recently reviewed the BCS model and described its relations to other parts of visual perception and to parts of visual cortex, this paper will only describe the model in general terms. The BCS' functional purpose is to identify the location and orientation of stimulus edges or boundaries. It accomplishes this by first feeding a visual image to simple cells, where each has a receptive field tuned to changes in luminance at a specific location and orientation. Signals from these cells contribute to complex cells that become insensitive to the direction of luminance change, but remain sensitive to orientation and position. These complex cells then feed into a series of cooperative and competitive hypercomplex cell stages that selects a consistent pattern of cell activations.

To aid contour detection, BCS complex cells pool responses from multiple scales. For the BCS model such pooled responses play an important role in computations of shading (Grossberg and Mingolla, 1987) and disparity (Grossberg, 1987, 1994,

1997; Grossberg and Marshall, 1989; Grossberg and McLoughlin, 1997). The details of disparity computations from cells of different spatial frequency sensitivities are complex and not directly relevant to the current discussion. For the moment simply consider the net activity feeding into a complex cell that pools data from cells of different spatial scales. To make the discussion more concrete, suppose that each (1D) oriented filter is a sine wave whose period exactly equals the filter's receptive field size and that each filter kernel is normalized so that the maximum response of each filter is the same value. Figure 1a shows the 1D kernels of such filters. Further suppose that the stimulus is a bar grating. With such filters and stimulus, a bar grating with a high fundamental frequency will generate a strong response among the small filters, which respond strongly to the edges of the bars. The larger scales will not respond nearly as strongly because the alternating bars will cancel out the

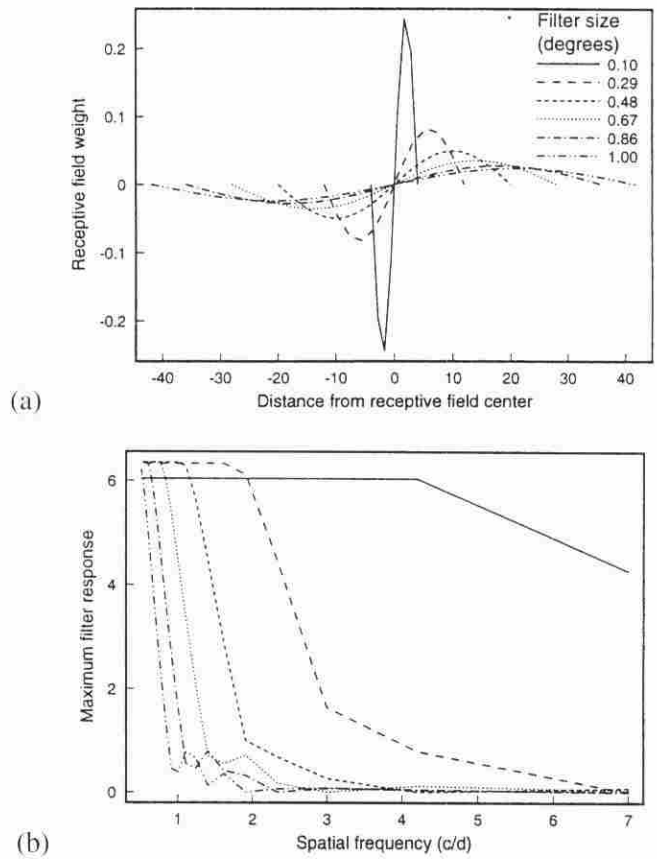

Figure 1. Properties for filters of different spatial scales. (a) One dimensional receptive field profiles. (b) Maximal response of each filter for square waves of different spatial frequencies. (c) The maximum sum of filter responses for different stimulus types. The sum of responses is inversely related to spatial frequency because more filters are tuned to low frequencies than high frequencies. (d) The maximum response of each filter for sine waves of different spatial frequencies. More filters are tuned to low than high spatial frequencies.

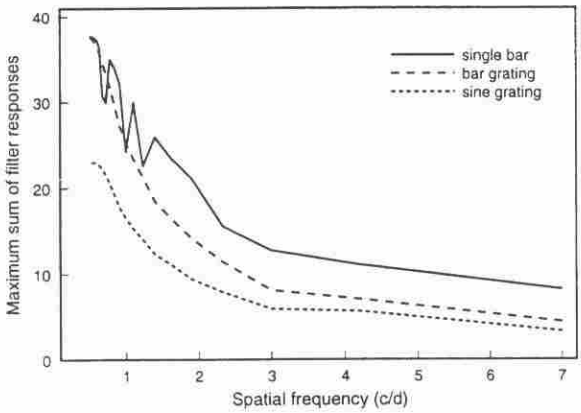

(c)

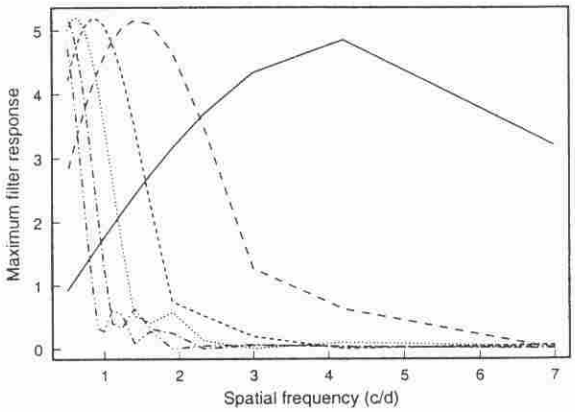

(d)

Figure 1. (Continued).

excitatory and inhibitory contributions to the filter. As a result, the sum of filter responses consists only of input from the smaller filters.

On the other hand, a bar grating with a lower fundamental frequency will excite both the large and small filters, as the latter respond to the sharp edges of the bars. As a result, the sum of filter responses is larger for the lower spatial frequency bar gratings. Figure 1b shows the maximal response of each filter in response to bar gratings of various fundamental frequencies. (The difference between filter responses for the lowest frequency stimuli is a side effect of pixel undersampling, and is unrelated to the arguments described below.) Figure 1c shows the maximal sum of responses for the bar gratings and other image types. (The jagged teeth are, again, due to pixel undersampling and have little bearing on the following arguments.) Consistent with the discussion above, the sum is inversely related to spatial frequency.

To understand the significance of this property for visual persistence requires a discussion of excitatory feedback and the role of reset signals in the BCS. In particular, the above analysis suggests that complex cells in the BCS give their

strongest responses to stimuli of the lowest spatial frequency. Studies of visual persistence find that low spatial frequency stimuli have the shortest persistence. Mistakenly equating persistence to a passive decay of neural activity suggests that persistence would increase with cell response. The next section describes an alternative account that is consistent with the psychophysical data.

BCS DYNAMICS

The responses of complex cells that pool across multiple spatial scales feed into a series of cooperative and competitive stages that identify the location and orientation of stimulus boundaries. A key component of this identification process is the use of excitatory feedback. The equilibrium response of the network will mostly include cells that send positive feedback to each other (directly or indirectly). Cells within an active excitatory feedback loop are said to have activities that *resonate*. Grossberg and Mingolla (1985a, b) showed that this excitatory feedback improves the network's ability to process spatial information.

The benefits of excitatory feedback for spatial processing come at a cost for temporal processing. The resonance generated by excitatory feedback loops dominates the temporal properties of the BCS. Simulations in Francis *et al.* (1994) demonstrated that, if left unchecked, resonating signals can last for hundreds of simulated milliseconds. To prevent resonating signals from lasting indefinitely, internal processes in the network automatically speed disappearance of persisting neural signals. Francis *et al.* (1994) identified two mechanisms embedded in the BCS design that reset activities in the feedback loop. One mechanism is lateral inhibition and its properties account for and predict many characteristics of visual masking, including effects on visual persistence (Francis *et al.*, 1994; Francis, 1996a), temporal integration (Francis, 1996b), and metacontrast masking (Francis, 1997).

The other mechanism is a type of cortical afterimage that resets persisting signals. Figure 2 schematizes separate pathways sensitive to the same position in visual space but perpendicular orientations. These pathways compete via reciprocal inhibition from lower levels to higher levels. Feeding this competition are inputs gated by habituative transmitters. Along with signals from external stimuli, each input pathway receives a tonic source of activity, and all output signals are rectified. This combination of rectification, opponent competition, habituative transmitter gates, and tonic input creates a gated dipole circuit (Grossberg, 1972). At the offset of stimulation, a gated dipole circuit generates a transient rebound of activity in the previously non-stimulated pathway.

The time plot next to each cell or gate in Fig. 2 describes the dynamics of this circuit. In the case shown, the sharp increase and then decrease of the time plot at the lower right indicates that an external input stimulates the horizontal pathway. In response to the stronger signal being transmitted to the next level, the amount of transmitter in the gate inactivates, or habituates, during stimulation and then rises

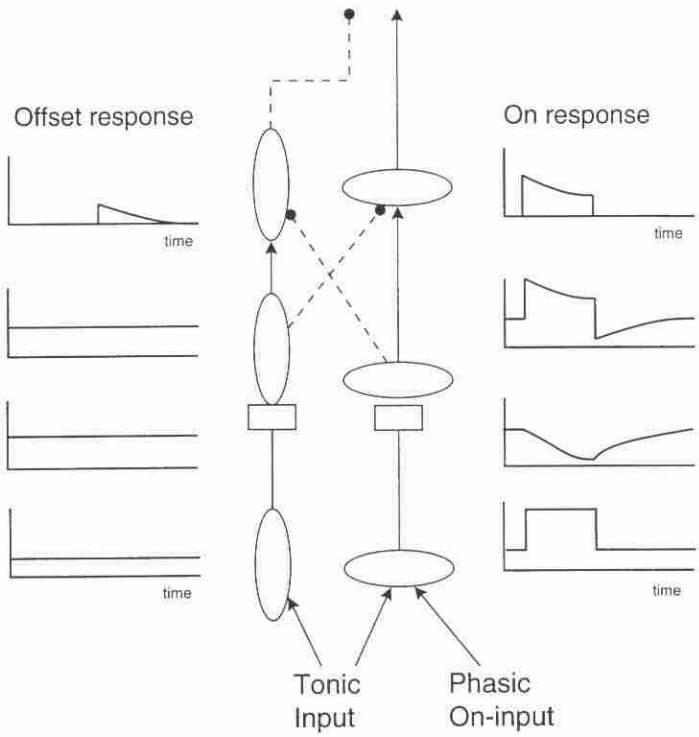

Figure 2. A schematic diagram of a gated dipole circuit with competition between orthogonal orientations. Solid lines indicate excitation and dashed lines indicate inhibition. Offset of a phasic horizontal input generates a rebound of activity in the vertical channel, which provides an inhibitory signal to higher level horizontal cells.

back toward the baseline level upon stimulus offset. Notice that the inactivation and reactivation of transmitter occur more slowly than changes in the activities of the neural cells. Each slowly habituating transmitter multiplies, or gates, the more rapidly varying signal in its pathway; thereby yielding net overshoots and undershoots at input onset and offset, respectively. During stimulation, the horizontal channel wins the rectified opponent competition against the vertical channel as indicated in the top right time plot. However, upon offset of the stimulation to the horizontal channel, the input signal returns to the baseline level but the horizontal transmitter gate remains habituated below its baseline value. As a result, shortly after stimulus offset, the gated tonic input in the horizontal channel has a net signal below the baseline level. Meanwhile, the vertical pathway maintains the baseline response at all cells and gates before the opponent competition. Thus, when the horizontal channel is below the baseline activity, after stimulus offset, the vertical channel wins the rectified opponent competition and produces a rebound of activity as shown in the top left time plot. As the horizontal transmitter gate recovers from its habituated state, the rebound signal in the vertical channel weakens and finally disappears. The duration

of the transient rebound thus matches the recovery rate of the transmitter from habituation.

A recent neurophysiological study of macaque monkeys demonstrates the existence of gated dipole circuits tuned for orientation in output layers of area V1. Ringach *et al.* (1997) explored dynamic changes in the orientation tuning curves of cells. They measured cell action potentials during rapid presentation of a series of sine gratings with different orientations. They then correlated action potentials with the grating orientations at successive times before each action potential. They found that action potentials correlated with one orientation after a short delay were also correlated with the orthogonal orientation after a longer delay. This finding is consistent with the properties of gated dipoles. The top vertically-oriented cell in Fig. 2 is sensitive to the presentation of a vertical edge, but it also responds to the offset of a horizontal edge. The delay between the horizontal edge offset and the vertical cell response corresponds to the time needed for the rebound signal to develop.

Ringach (1998) recently used a variation of this experiment on human subjects who reported as quickly as possible when they saw a target orientation. The data did not allow a full description of the temporal aspects of orientation detection, but subjects were more likely to report seeing the target orientation when either the target orientation or its orthogonal orientation was presented than for any other stimulus. These results are consistent with an orientational rebound generated by the offset of an orthogonal orientation. Additional psychophysical evidence of orientationally tuned gated dipoles comes from studies of orientational afterimages. MacKay (1957) noted that fixation of a set of concentric, high contrast, circles could lead to a streaming radial afterimage. Francis and Grossberg (1996b) explained how the gated dipole rebounds generated by MacKay's images could lead to a new visual segmentation to produce the afterimage.

The gated dipole circuit is part of a larger BCS circuit that determines the location and orientation of stimulus boundaries using positive feedback. In this neural circuit, an orientationally sensitive cell is excited by cells of the same orientation sensitivity and inhibited by cells of the orthogonal orientation sensitivity. Thus, the rebound generated by the gated dipole circuit inhibits any persisting activity generated by the oriented edges of the stimulus.

The properties of reset signals explain the inverse duration and inverse intensity effects for persistence duration (Francis *et al.*, 1994) and temporal integration (Francis, 1996b). They also explain why the persistence of illusory contours is greater and differently affected by stimulus duration than luminance contours (Meyer and Ming, 1988; Francis *et al.*, 1994). In each case, stimuli that produce a strong response among oriented cells feeding into the gated dipole generate a strong reset signal at stimulus offset. The strong reset signal greatly reduces persistence. Weaker stimuli (smaller luminance, shorter duration, fewer luminance contours) produce smaller reset signals at stimulus offset, thereby allowing persisting neural signals to last longer.

More direct evidence that orientational reset signals underlay visual persistence comes from a study by Meyer *et al.* (1975) that demonstrated orientation specific adaptation effects. In this study subjects adapted to a bar grating of either vertical or horizontal orientation. Persistence measurements for bar gratings were then gathered. When subjects adapted to a stimulus of the same orientation as the test stimulus, persistence of the test stimulus decreased, relative to a no adaptation measurement; but when subjects adapted to a stimulus of a perpendicular orientation to the test stimulus, persistence of the test stimulus increased. These properties are consistent with the model. Adaptation to, say, a horizontal stimulus habituates the transmitter in horizontal pathways but leaves the vertical pathways unadapted. If one then tests persistence of a horizontal stimulus, the horizontal pathways further habituate transmitter during the test presentation. The stronger than usual habituation of the horizontal pathways means that, at stimulus offset, the reset signals will be stronger than usual and persistence will decrease. On the other hand, if one tests persistence of a vertical stimulus, then both oriented pathways become habituated: the horizontal pathways from the prior adaptation and the vertical pathway from the habituation due to the target presentation. As a result of the opponent competition between these habituated signals (Fig. 2), the reset signals generated at offset of the vertical test stimulus will be weaker than usual and persistence will increase.

The properties of the gated dipole also explain the effects of spatial frequency for bar gratings. As spatial frequency increases, the larger oriented filters respond less strongly and the response of the pooling complex cell decreases. With a weaker response there is less transmitter depletion and a weaker reset signal. With a weaker reset signal, the persisting neural trace lasts longer, thereby leading to longer visual persistence. Simulations in the next section demonstrate that this proposal accounts for psychophysical data.

Before turning to the simulations though, it is necessary to consider whether the response bias for lower spatial frequency bar gratings generalizes to sine gratings. In contrast to its response for bar gratings, the response of the smallest filter decreases for low spatial frequency sine gratings because there is less change in contrast across its receptive field. There are at least three situations that would generate a response bias for sine gratings of lower spatial frequency.

First, cells that act as low pass filters require a larger receptive field than cells that act as high pass filters. With a larger receptive field it may be that the low-pass cells are able to integrate more total energy and so give a stronger maximum response than the smaller high-pass cells. Two neurophysiological studies are partly consistent with this view. De Valois *et al.* (1982) measured contrast sensitivity to drifting gratings for macaque striate cortical cells. Contrast sensitivity was the reciprocal of the grating contrast needed to reach a specified criterion response. Those cells sensitive to low frequency gratings had larger contrast sensitivity than cells sensitive to high frequency gratings. In earlier work in cat visual cortex, Maffei and Fiorentini (1973) showed a weak trend for average discharges to be

directly related to cell receptive field size. The data are far from conclusive as each study described only a few cells. There is less data than would be expected on this issue because when reporting cell firing rates, it is customary to normalize responses relative to a cell's maximum firing rate. Nevertheless, if it was true that cells sensitive to low spatial frequencies had stronger responses than cells sensitive to high spatial frequencies, a complex cell that summed across spatial scales would respond more strongly to low frequency sine waves than to high frequency sine waves.

Second, it could be that more cells are tuned to lower frequencies than high frequencies. Studies of area V2 in macaque monkey show that a large percentage of the cells prefer low spatial frequencies (Foster *et al.*, 1985; Levitt *et al.*, 1994). This is also true for the filters in Fig. 1. Figure 1d plots the maximum response of each filter for sine gratings of various frequencies; only one filter is sensitive to the highest frequencies but many filters are sensitive to the lower frequencies. This bias to sampling low frequencies is a natural consequence of constant increases in receptive field size. When receptive field size is converted to spatial frequency sensitivity, the constant size increase corresponds to relatively small sensitivity changes in frequency. The result is that the sum of filter responses contains signals from more low frequency tuned filters than high frequency tuned filters and shows a stronger response to low frequency sine waves than to high frequency sine waves. Figure 1c demonstrates this response bias for sine gratings, bar gratings, and single bars.

Third, competition at stages beyond the oriented filters may favor the larger scale cells and lower frequencies. In Grossberg's FACADE theory (1994, 1997), the large scale cells are able to fuse larger disparities than the small scale cells, and in subsequent competitions there is a bias for larger disparities. In many contexts, this disparity bias translates into a low spatial frequency bias.

The following simulations use the second method to create a response bias for low frequency sine gratings. This is primarily because it is the simplest method to implement and requires the least computational burden. Moreover, the neurophysiology supports the notion that there are more cells tuned to low frequencies than high frequencies in area V2 of monkey cortex. The simulation is not, however, attempting to formally model the receptive fields of visual cells in monkey cortex. Instead, the simulation is capturing a general property that seems to be consistent with neurophysiological data.

SIMULATIONS

The Appendix provides details of the equations and cell receptive fields. Each simulation emulated a one-dimensional cross-section of a visual image and cell receptive fields. The simulations demonstrate how the properties of spatial scale, gated dipoles, and persisting neural signals account for psychophysical data. The nature of the account is necessarily qualitative rather than quantitative because the

data derive from different subjects and methodologies. Subject differences can be substantial (persistence differences of hundreds of milliseconds) and attempting to account for subject differences would introduce so many free parameters as to hide the fundamental model characteristics that underlay the basic effects. Instead, all simulations used a fixed set of equations and parameters, with the understanding that a precise fit to experimental data is not to be expected. As a result, success of the simulations should be measured by their ability to match the robust trends of the data rather than their ability to provide a quantitative fit to data values. In general, the simulated results are not far from what would be expected for a subject in an experiment.

Spatial frequency and stimulus size

Figure 3a plots data from Meyer and Maguire (1977, 1979) demonstrating the effect of spatial frequency on visual persistence. The two experiments were similar in experimental technique and varied mostly in stimulus type. In each case a blank screen with a variable interstimulus interval (ISI) separated two 50 ms flashes of a stimulus (bar grating, sine grating, or single bar). The observer commented on whether a clear blank field seemed to separate the two flashes. The experimenter adjusted the ISI to find the value at which the percept changed from continuity to discontinuity, and this ISI was taken as a measure of persistence. This measure tends to provide longer estimates of persistence than other methods (Meyer and Maguire, 1979), but otherwise shows the same qualitative behavior. In Meyer and Maguire (1977) the stimulus was a square wave grating of various frequencies. In Meyer and Maguire (1979) the stimulus was either a sine wave grating or a single bar from a bar grating. Figure 3a shows, for a representative observer (one of the authors, who participated in both experimental studies), that persistence increased by nearly 200 ms as spatial frequency increased from 0.4 to 15 cyc/deg. This basic effect was true for all types of stimuli. Other studies have reported similar effects of spatial frequency (e.g. Bowling *et al.*, 1979; Di Lollo and Woods, 1981; Long and Gildea, 1981).

The model explains the effect of spatial frequency through interactions of multiple sized oriented filters and the properties of the gated dipole. As Fig. 1c demonstrates, the maximal summed response among the filters is stronger for lower spatial frequency stimuli. Such stimuli also generate the strongest inhibitory rebounds at stimulus offset, which more strongly inhibit persisting responses. As simulation results in Fig. 3b show, this general property does not depend on the type of stimulus used. In each simulation, the stimulus luminance, contrast, and duration were the same as in the corresponding experimental study.

Frequency and duration

Figure 4a plots data from Meyer and Maguire (1981) demonstrating an interaction between spatial frequency and target duration. Using the same methodological

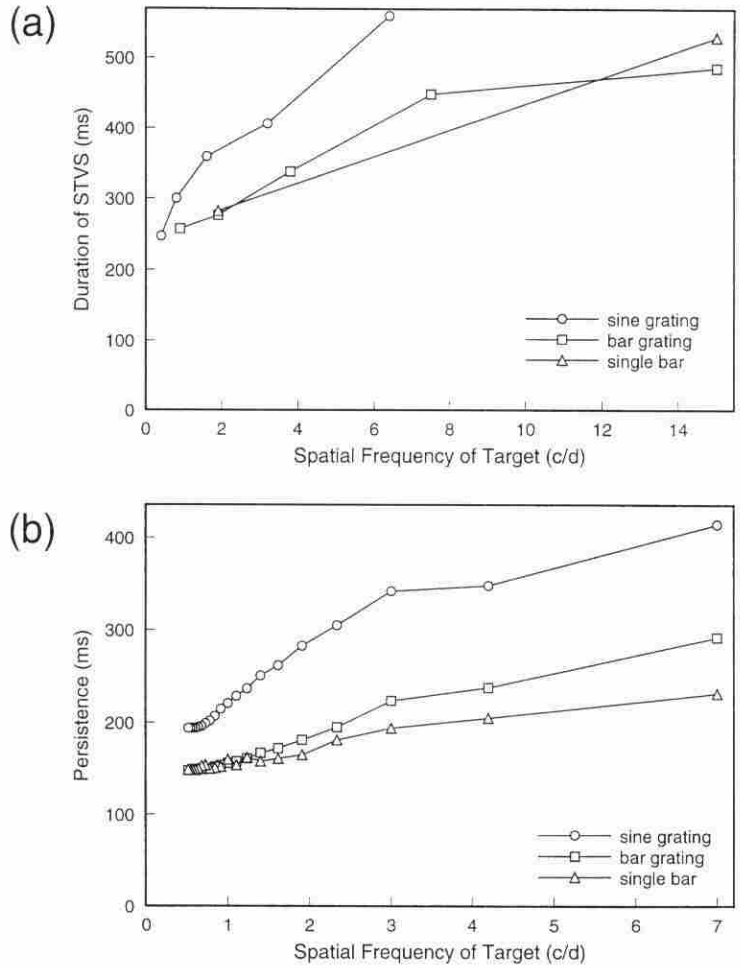

Figure 3. Persistence is directly related to spatial frequency. This basic effect is true for sine gratings, bar gratings, and individual bars. (a) Psychophysical data from Meyer and Maguire (1977, 1979). STVS stands for Short Term Visual Store, which is equivalent to visual persistence. (b) Simulation data.

technique as in Meyer and Maguire (1977), they varied the duration and spatial frequency of the target. As expected, persistence decreased as target duration increased and increased for higher spatial frequencies. Notably though, the inverse duration effect was much smaller for the low spatial frequency gratings than for the high spatial frequency grating.

This experimental finding is consistent with the model's explanation. The duration of persistence is inversely related to the strength of the rebound generated at stimulus offset. The rebound strength is determined by the strength and duration of the signal passing through the depletable transmitter gate. A relatively weak signal shows marked differences for stimuli of different durations, while a strong signal quickly depletes the gate so that further increases in stimulus duration have little

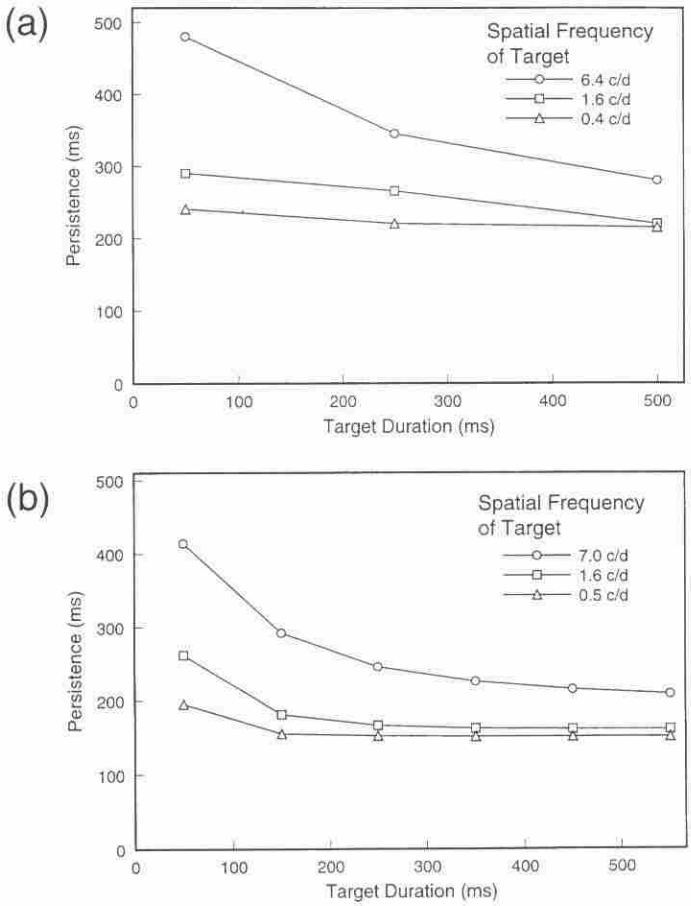

Figure 4. An interaction of spatial frequency and target duration on visual persistence duration. The high spatial frequency grating shows a strong inverse-duration effect, while the low spatial frequency gratings show weak effects of target duration. (a) Psychophysical data from Meyer and Maguire (1981). (b) Simulation data.

effect. Such is the case for the simulations that generated the data in Fig. 4b. The high frequency stimulus provides a relatively weak signal that shows marked effects of stimulus duration, while the low frequency stimuli provide strong signals that quickly deplete the gate and extended target durations provide no further depletion. The different asymptotic persistence values reflect differences in the strength of the signal depleting the gate. A weak signal cannot deplete the gate as fully as a strong signal, regardless of target duration.

Pretest adaptation

Additional support for the role of habituation-based reset signals comes from a second experiment by Meyer and Maguire (1981). The stimuli were nearly identical to those in the investigation of duration effects, but before measuring persistence

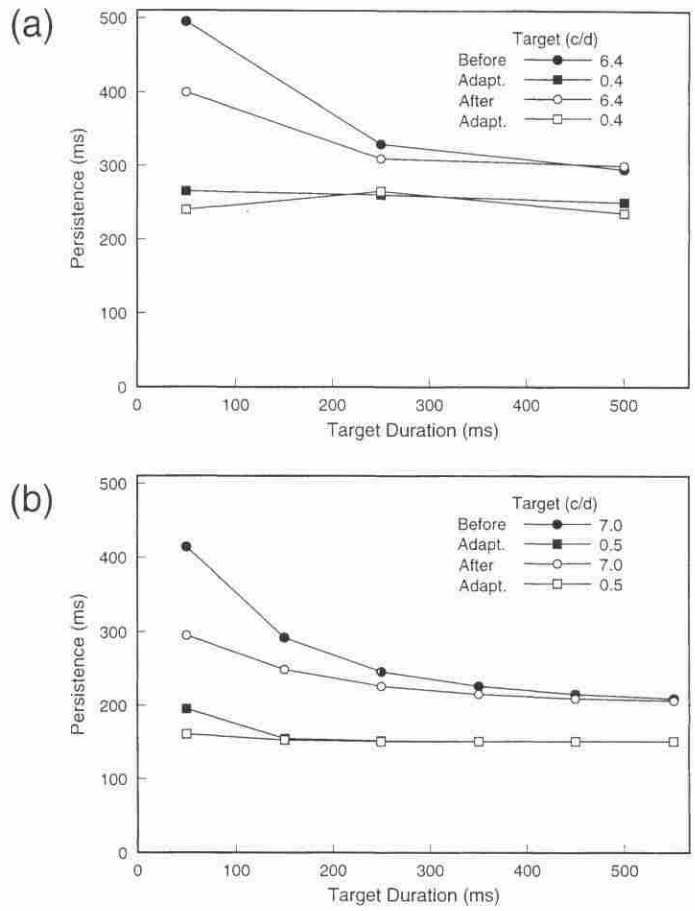

Figure 5. Preadaptation to the test grating reduces persistence of the short duration, high frequency, stimulus, but not long duration or low frequency stimuli. (a) Psychophysical data from Meyer and Maguire (1981). (b) Simulation data.

subjects adapted for three minutes to either a blank field or a grating of the same spatial frequency as would be tested. Figure 5a shows the difference of adaptation type for two target spatial frequencies and three durations. The high spatial frequency gating has a smaller persistence for the 50 ms duration, but not for the longer durations. The low frequency grating shows no difference for adaptation type.

These findings are consistent with the model's explanation of spatial frequency and stimulus duration interactions, as simulation results in Fig. 5b demonstrate. During adaptation to a grating, the habituating gates become depleted and the depletion can produce stronger than normal reset signals at target stimulus offset, thereby reducing target persistence. At the long durations, both the low and high frequency target gratings deplete the habituating gate to their respective maximum amounts, so the type of adaptation has no effect on the total habituation or the

strength of the reset signal. As a result, persistence is unchanged for long target durations. For short target durations, the strong signal from a low frequency grating again fully depletes the gate, so adaptation to a grating has no noticeable effect. For the high frequency grating at a short duration, the weaker signal passing through the gate does not fully deplete the gate for the blank adaptation condition. As a result, the effects of habituation during grating adaptation can be observed.

It should be noted that a second adaptation study by Meyer and Maguire (1979) offers further challenges. Their study was similar to the one above, but they fixed target duration and varied target spatial frequency. They found that persistence decreased most for a test grating of the same frequency as the adaptation grating. Some target gratings with frequencies different from the adaptation grating showed an increase in persistence. Current simulations cannot account for this result, as the adaptation stimulus always decreases persistence, if it has any effect. The simulations also systematically show that adaptation to a grating has a big effect on test gratings of higher spatial frequency, while the data do not show this effect.

While these data are problematic for the current simulations, it is plausible that model characteristics not included in the current simulations can account for these results. The frequency-specific adaptation data suggest that there is a competition between cells of different spatial scales. This competition is part of Grossberg's (1994, 1997) theory of depth segmentation called FACADE (Form And Color And DEpth), which uses signals from oriented signals of multiple scales to compute disparity. If gated dipoles are placed appropriately in those competitions, FACADE may be able to account for frequency-specific adaptation effects on visual persistence. A full dynamic simulation of FACADE theory is prohibited by the enormous computation involved in working with many non-linear differential equations and parameter estimations. As equations that describe FACADE interactions are defined by other model constraints, it will be important to determine whether the model's dynamic properties also account for the frequency-specific effects of adaptation on persistence.

Residual traces

As noted in the introduction, a commonly found property of visual persistence is that it is inversely related to stimulus duration and luminance and directly related to stimulus spatial frequency. However, there exist a set of studies that purport to show opposite relationships. Figure 6a replots data from Long and Sakitt (1981) showing an inverse relationship between persistence and spatial frequency. In this study the experimenter, set the ISI between a target bar grating and a small probe stimulus so that the probe appeared just as *all trace* of the target disappeared. This critical ISI value was the measure of persistence. The instructions to the subject differ from the studies of Meyer and Maguire, who asked the subject to report when they saw the target turn on and off. Apparently, there can be traces of a visual percept even though subjects report seeing it turn off. With the emphasis on observing

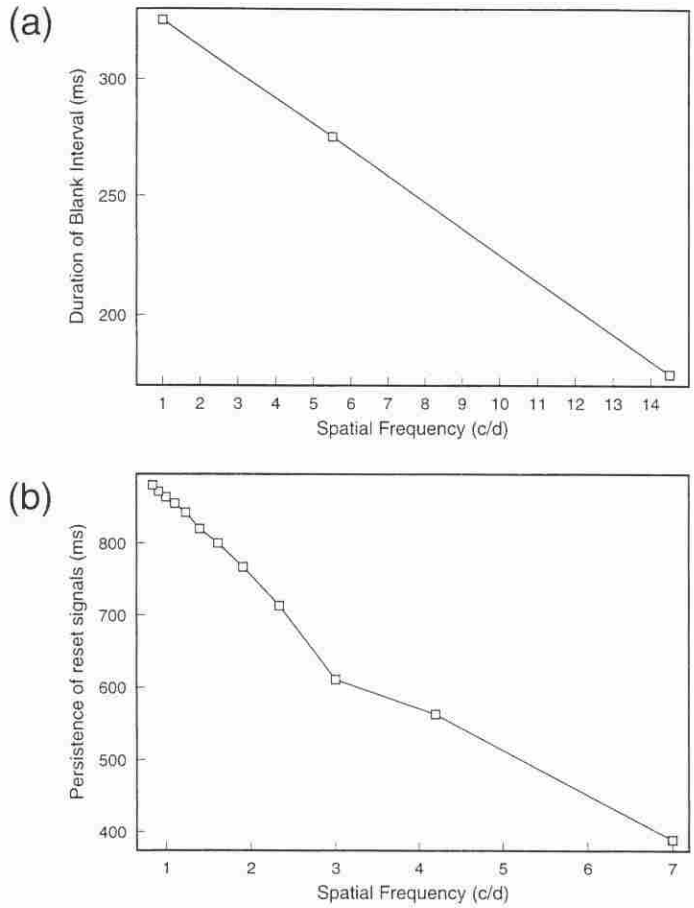

Figure 6. Duration of residual traces is inversely related to spatial frequency. (a) Psychophysical data from Long and Sakitt (1981). (b) Simulation data.

any residual trace of the target stimulus, studies of this type find that persistence is directly related to stimulus luminance and duration (e.g. Long and McCarthy, 1982).

The different effects of stimulus luminance, duration, and spatial frequency on persistence and residual traces have been the basis for heated discussion about experimental methods and data interpretation (Long, 1980; Irwin and Yeomans, 1986; Nisly and Wasserman, 1986; Di Lollo and Bischof, 1995). Francis and Grossberg (1996) proposed a partial resolution to the controversy by hypothesizing that awareness of residual traces could include awareness of the reset signals generated by gated dipoles in the BCS. With this hypothesis, the reason persistence is inversely related to stimulus duration and luminance and directly related to spatial frequency is linked to the reason residual traces are oppositely related to the same variables. Lower spatial frequency stimuli lead to stronger oriented responses, more substantial depletion of transmitter, and stronger rebounds in the gated dipole

circuits. Because the transmitter recovers at a fixed rate, stronger rebounds last longer, thereby leading to an inverse relationship between residual trace duration and spatial frequency.

Figure 6b shows simulation results demonstrating the inverse relationship between residual trace duration and spatial frequency. These simulations measured the time from stimulus offset to the time when all cell responses were below a fixed threshold. Because these measurements included cell activities generated by gated dipole rebounds, they decrease with spatial frequency.

The durations of residual traces generated by the model are quantitatively larger than the data in Fig. 6a. A different set of parameters could generate a better fit, but at the cost of the fit to the data in Figs 3 and 4. In the model, the duration of residual traces must be greater than or equal to the duration of persistence. This is not the case in the experimental data where different methods find quite different measures of persistence and residual trace durations. The Long and Sakitt experiment uses a different methodology than the persistence studies, and it is likely that subjects adopted different criteria for judging persistence. The current simulations do not attempt to explain differences in experimental measures.

DISCUSSION

When they first noted the effect of spatial frequency on persistence, Meyer and Maguire (1977) suggested that it was due to the spatio-temporal differences between transient and sustained channels. The transient channels would be more sensitive to lower spatial frequencies and have faster dynamic responses, hence shorter persistence. There may be some truth to this theory, but it leaves unexplained many other properties of visual persistence, including the inverse duration and luminance effects, residual traces, effects of orientation-specific adaptation, and persistence of illusory contours.

The BCS model provides a parsimonious account of all these data sets. In addition the BCS theory explains properties of temporal integration (Francis, 1996b), metacontrast masking (Francis, 1997), apparent motion (Francis and Grossberg, 1996a), and oriented afterimages (Francis and Grossberg, 1996b). Thus, the BCS model provides a unified account of many psychophysical data related to dynamic vision. Even more significant is the observation that none of the model mechanisms are supported solely by data from dynamic vision. Each stage of processing in the model is additionally supported by psychophysical data on brightness perception (Grossberg and Todorović, 1987), form perception (Grossberg and Mingolla, 1985b) and figure-ground separation (Grossberg, 1997), among others. The BCS model is currently the only theory of visual perception with such far-reaching explanatory power.

REFERENCES

Bowen, R., Pola, J. and Matin, L. (1974). Visual persistence: Effects of flash luminance, duration and energy, *Vision Research* **14**, 295–303.

Bowling, A., Lovegrove, W. and Mapperson, B. (1979). The effect of spatial frequency and contrast on visual persistence, *Perception* **8**, 529–539.

De Valois, R. L., Albrecht, D. G. and Thorell, L. G. (1982). Spatial frequency selectivity of cells in macaque visual cortex, *Vision Research* **22**, 545–559.

Di Lollo, V. and Bischof, W. (1995). The inverse-intensity effect in duration of visible persistence, *Psychological Bulletin* **118**, 223–237.

Di Lollo, V. and Woods, E. (1981). Duration of visible persistence in relation to range of spatial frequencies, *Journal of Experimental Psychology: Human Perception and Performance* **7**, 754–769.

Farrell, J., Pavel, M. and Sperling, G. (1990). The visible persistence of stimuli in stroboscopic motion, *Vision Research* **30**, 921–936.

Foster, K., Gaska, J., Nagler, M. and Pollen, D. (1985). Spatial and temporal frequency selectivity of neurons in the visual cortical areas V1 and V2 of the macaque monkey, *Journal of Physiology* **365**, 331–363.

Francis, G. (1996a). Cortical dynamics of lateral inhibition: Visual persistence and ISI, *Perception and Psychophysics* **58**, 1103–1109.

Francis, G. (1996b). Cortical dynamics of visual persistence and temporal integration, *Perception and Psychophysics* **58**, 1203–1212.

Francis, G. (1997). Cortical dynamics of lateral inhibition: Metacontrast masking, *Psychological Review* **104**, 572–594.

Francis, G. and Grossberg, S. (1996a). Cortical dynamics of form and motion integration: Persistence, apparent motion, and illusory contours, *Vision Research* **36**, 149–174.

Francis, G. and Grossberg, S. (1996b). Cortical dynamics of boundary segmentation and reset: Persistence, afterimages, and residual traces, *Perception* **25**, 543–567.

Francis, G., Grossberg, S. and Mingolla, E. (1994). Cortical dynamics of feature binding and reset: Control of visual persistence, *Vision Research* **34**, 1089–1104.

Grossberg, S. (1972). A neural theory of punishment and avoidance: II. Quantitative theory, *Mathematical Biosciences* **15**, 253–285.

Grossberg, S. (1987). Cortical dynamics of three-dimensional form, color, and brightness perception II: Binocular theory, *Perception and Psychophysics* **41**, 117–158.

Grossberg, S. (1994). 3-D vision and figure-ground separation by visual cortex, *Perception and Psychophysics* **55**, 48–120.

Grossberg, S. (1997). Cortical dynamics of three-dimensional figure-ground perception of two-dimension pictures, *Psychological Review* **104**, 618–658.

Grossberg, S. and Marshall, J. (1989). Stereo boundary fusion by cortical complex cells: A system of maps, filters, and feedback networks for multiplexing distributed data, *Neural Networks* **2**, 29–51.

Grossberg, S. and McLoughlin, N. (1997). Cortical dynamics of 3-D surface perception: Binocular and half-occluded scenic images, *Neural Networks* **10**, 1583–1605.

Grossberg, S. and Mingolla, E. (1985a). Neural dynamics of form perception: Boundary completion, illusory figures, and neon color spreading, *Psychological Review* **92**, 173–211.

Grossberg, S. and Mingolla, E. (1985b). Neural dynamics of perceptual grouping: Textures, boundaries, and emergent segmentations, *Perception and Psychophysics* **38**, 141–171.

Grossberg, S. and Todorović, D. (1988). Neural dynamics of 1-D and 2-D brightness perception: A unified model of classical and recent phenomena, *Perception and Psychophysics* **43**, 241–277.

Irwin, D. E. and Yeomans, J. M. (1986). Persisting arguments about visual persistence: Reply to Long, *Perception and Psychophysics* **39**, 225–230.

Levitt, J. B., Kiper, D. C. and Movshon, J. A. (1994). Receptive fields and functional architecture of macaque V2, *Journal of Neurophysiology* **71**, 2517–2542.

Long, G. (1980). Iconic memory: A review and critique of the study of short-term visual storage, *Psychological Bulletin* **88**, 785–820.
Long, G. and Gildea, T. (1981). Latency for the perceived offset of brief target gratings, *Vision Research* **21**, 1395–1399.
Long, G. and McCarthy, P. (1982). Target energy effects on Type I and Type II visual persistence, *Bulletin of the Psychonomic Society* **19**, 219–221.
Long, G. and Sakitt, B. (1981). Differences between flicker and non-flicker persistence tasks: The effects of luminance and the number of cycles in a grating target, *Vision Research* **21**, 1387–1393.
MacKay, D. (1957). Moving visual images produced by regular stationary patterns, *Nature* **180**, 849–850.
Maffei, L. and Fiorentini, A. (1973). The visual cortex as a spatial frequency analyser, *Vision Research* **13**, 1255–1267.
Meyer, G., Lawson, R. and Cohen, W. (1975). The effects of orientation-specific adaptation on the duration of short-term visual storage, *Vision Research* **15**, 569–572.
Meyer, G. and Maguire, W. (1977). Spatial frequency and the mediation of short-term visual storage, *Science* **198**, 524–525.
Meyer, G. and Maguire, W. (1979). The effects of bar width and spatial frequency-specific adaptation on visual persistence, *Bulletin of the Psychonomic Society* **14**, 64–66.
Meyer, G. and Maguire, W. (1981). Effects of spatial-frequency specific adaptation and target duration on visual persistence, *Journal of Experimental Psychology: Human Perception and Performance* **7**, 151–156.
Meyer, G. and Ming, C. (1988). The visible persistence of illusory contours, *Canadian Journal of Psychology* **42**, 479–488.
Nisly, S. and Wasserman, G. (1989). Intensity dependence of perceived duration: Data, theories, and neural integration, *Psychological Bulletin* **106**, 483–496.
Ringach, D. L., Hawken, M. J. and Shapley, R. (1997). Dynamics of orientation tuning in macaque primary visual cortex, *Nature* **387**, 281–284.
Ringach, D. L. (1998). Tuning of orientation detectors in human vision, *Vision Research* **38**, 963–972.

APPENDIX: SIMULATION DETAILS

Each one-dimensional simulation consisted of three hundred pixels that correspond to a cross-section of a larger image plane. On this image line, the image intensity at pixel i of a luminance grating was described by the function

$$I_i = L\left[1 + C\sin\left(\frac{i\pi}{S}\right)\right], \tag{1}$$

where L was the mean luminance of the grating, C was the contrast, and S was the number of pixels in a half cycle of the grating.

At each pixel location, six pairs of filters (six different sizes, two directions of contrast change) were convolved with the image. Each filter was described by an equation of the form

$$F_{kd} = \frac{1}{2(4+8d)}\sin\left(\frac{k\pi}{4+8d}\right), \tag{2}$$

where k is the distance from the filter center and $4 + 8d$ is the number of the pixels in a half-cycle of the filter. The division by $2(4 + 8d)$ normalizes the grating so that

deviations from zero summed to one regardless of filter size. Filter sizes ranged from $d = 0$, with a half cycle of 4 pixels, to $d = 5$, with a half cycle of 44 pixels. The resulting kernels are plotted in Fig. 1a. A complementary set of filters, $G_{kd} = -F_{kd}$ detected luminance changes from bright to dark.

The responses of the filters were combined to generate response properties analogous to complex cells in visual cortex. The activity of a simulated complex cell at position i was calculated as:

$$C_i = \sum_{d=0}^{5} \left\{ \left[\sum_{k=-(4+8d)}^{4+8d} F_{kd} I_{(i+k)} \right]^+ + \left[\sum_{k=-(4+8d)}^{4+8d} G_{kd} I_{(i+k)} \right]^+ \right\}. \tag{3}$$

Here each inner sum convolves a filter with the image plane, and the outer sum adds up the resulting value of the convolutions across all filter sizes. The notation $[\ ]^+$ indicates half-wave rectification. The maximum C_i value across the image line is plotted in Fig. 1c for different image types and spatial frequencies.

The C_i activities fed into a gated dipole circuit. At each pixel location a habituating gate obeys the differential equation

$$\frac{\mathrm{d}H_i}{\mathrm{d}t} = P\big[A - H_i - (B + EC_i)H_i\big]. \tag{4}$$

Here parameter $P = 0.01$ insures that the gate changes at a rate slower than the differential equations describing neural activities. The term $A - H_i$ describes recovery of neurotransmitter, while the term $-(B + EC_i)H_i$ describes depletion of neurotransmitter due to signal passing through the cell. Parameter $A = 100$ establishes an upper amount of neurotransmitter available; parameter $B = 1$ is the tonic signal passing through each parallel pathway of the gated dipole; parameter $E = 4$ scales the response of complex cells. For each simulation H_i is initialized to the equilibrium reached when only the tonic input depletes the gate.

$$H_i(0) = \frac{A}{1 + B}. \tag{5}$$

The next computation in the simulation collapses the excitatory and inhibitory components of the gated dipole into a single equation. The output value of a gated dipole at position i is

$$M_i = (B + EC_i)H_i(t) - BH_i(0), \tag{6}$$

which subtracts the gated tonic signal from the gated signal during stimulation. The value subtracted is identical to what would be subtracted by an unstimulated opponent pathway in a gated dipole circuit.

The next computation in the simulation collapses the feedback dynamics in the BCS to a single set of equations that capture many of the same dynamic properties. The M_i values input to hypercomplex cells that exhibit substantial persistence at

stimulus offset. Each hypercomplex cell activity obeys the differential equation

$$\frac{dY_i}{dt} = -RY_i + (Q - Y_i)[M_i]^+ - T[-M_i]^+. \quad (7)$$

Here $R = 0.04$ sets the rate of passive decay to be small so that there is substantial persistence even when the M_i values equal zero. Parameter $Q = 1$ establishes an upper limit to the value of Y_i. The second term describes shunting excitation resulting when M_i is positive. The last term describes subtractive inhibition when M_i is negative (i.e. during a gated dipole rebound). The parameter $T = 0.001$ scales the strength of the inhibitory reset signal.

Persistence was measured as the time between stimulus offset and the time when any of the Y_i values dropped below the fixed threshold of 0.1. For the simulations measuring the duration of residual traces, a hypercomplex cell sensitive to the reset signal and inhibited by the original input signals obeyed the differential equation

$$\frac{dZ_i}{dt} = -RZ_i + (Q - Z_i)[-M_i]^+ - T[M_i]^+, \quad (8)$$

and residual trace duration was measured as the time between stimulus offset and the time when all Z_i values dropped below the fixed threshold of 0.995.

In each simulation the luminance, contrast, and duration of the simulated stimulus is the same as in the corresponding psychophysical stimulus. Simulated luminance values are treated as foot-lambert values, and a simulated time unit corresponds to 10 ms. When converting pixel images to spatial frequencies, one deg of visual angle is scaled to the distance separating 42 pixels.

Simulations of the adaptation study deserve special note. Emulating the precise adaptation procedure used by Meyer and Maguire (1981) would be complicated because they had subjects adapt for three min and subjects undoubtedly moved their eyes over the stimulus. Matching these properties in the simulation would require substantial computing time, so a more tractable alternative was used. During an adaptation period, a grating stimulus was presented for 200 ms and then followed by a blank image for 50 ms. To emulate the effects of eye movements, all habituating gates were then initialized to the spatial average of the habituating gates at the end of the blank image presentation. With the habituation gates initialized to the adaptation values, the remainder of the simulation was unchanged. One prediction of this model property is that the extensive adaptation used by Meyer and Maguire is not necessary, provided the target is presented soon after offset of the adapting stimulus.